Iron Oxide Nanoparticle-Induced Epidermal Growth Factor Receptor Expression in Human Stem Cells for Tumor Therapy

Tsai-Hua Chung,[†,⊥] Jong-Kai Hsiao,[‡] Szu-Chun Hsu,[§] Ming Yao,[#] Yao-Chang Chen,[§,#,*] Shih-Wei Wang,[∥] Mark Yen-Ping Kuo,[⊥] Chung-Shi Yang,[†] and Dong-Ming Huang[†,*]

[†]Center for Nanomedicine Research, National Health Research Institutes, Miaoli, Taiwan, Republic of China, [⊥]Graduate Institute of Clinical Dentistry School of Dentistry, National Taiwan University Hospital and College of Medicine, National Taiwan University, Taipei, Taiwan, Republic of China, [‡]Department of Medical Imaging, Buddhist Tzu Chi General Hospital, Taipei Branch and School of Medicine, Tzu Chi University, Taiwan, Republic of China, [§]Department of Laboratory Medicine, National Taiwan University Hospital and College of Medicine, National Taiwan University, Taipei, Taiwan, Republic of China, [#]Department of Internal Medicine, National Taiwan University Hospital and College of Medicine, National Taiwan University, Taipei, Taiwan, Republic of China, and [∥]Department of Medicine, Mackay Medical College, New Taipei City, Taiwan, Republic of China

ABSTRACT

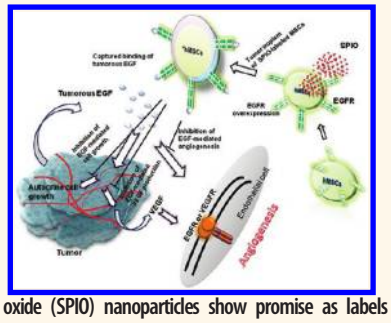

Superparamagnetic iron oxide (SPIO) nanoparticles show promise as labels for cellular magnetic resonance imaging (MRI) in the application of stem cell-based therapy. However, the unaddressed concerns about the impact of SPIO nanoparticles on stem cell attributes make the feasibility of SPIO labeling uncertain. Here, we show that the labeling of human mesenchymal stem cells (hMSCs) with ferucarbotran can induce epidermal growth factor receptor (EGFR) overexpression. Labeled hMSCs with their overexpressed EGFR were attracted by tumorous EGF and more effectively migrated toward tumor than unlabeled cells, resulting in more potent intrinsic antitumor activity. Moreover, the captured binding of tumorous EGF by overexpressed EGFR of labeled hMSCs blocked EGF/EGFR signaling-derived tumor growth, tumorous angiogenesis, and tumorous VEGF expression also responsible for tumor progression and development. Our results show that the impact of SPIO nanoparticles on stem cell attributes is not necessarily harmful but can be cleverly used to be beneficial to stem cell-based therapy.

KEYWORDS: iron oxide nanoparticle · mesenchymal stem cell · tumor tropism · MRI · cancer therapy

Stem cells, with their differentiation and tropism/homing capacities, can be utilized for regenerative therapy and treatment of several diseases, including human malignancies. Development of this stem cell-based therapy requires monitoring the fate and distribution of transplanted cells to maximize the therapeutic benefit. Up to now, superparamagnetic iron oxide (SPIO) nanoparticles appear to be the most applicable probe to label stem cells for cellular magnetic resonance imaging (MRI), which has afforded superb spatial resolution and repeated noninvasive imaging of magnetically labeled cells *in vivo*. However, the impact of SPIO nanoparticles on stem cell attributes remains an unresolved issue.[1−5] Although a number of studies have concluded the feasibility of stem cell labeling with SPIO nanoparticles, growing evidence shows that cellular responses to SPIO labeling were indeed observed.[6−8] These somewhat controversial conclusions might be due to the used cell types and culture conditions, various iron oxide particles and labeling methods, and criteria for evaluating the impact of SPIO nanoparticles in different studies. Furthermore, the conclusion of the feasibility of using SPIO nanoparticles would be complicated by the mission of transplanted stem cells.

For instance, in our previous studies ferucarbotran (Resovist), an ionic SPIO nanoparticle with carboxydextran coating, has been shown to be able to activate the migration and hence to block osteogenesis of human mesenchymal stem cells (hMSCs),[3] suggesting the need for caution about using ferucarbotran to label stem cells for osteogenic MRI tracking. However, a higher expression of chemokine receptor CXCR4 was induced in ferucarbotran−protamine complex-labeled hMSCs and was suggested to contribute to an increased stem cell migration toward glioma cells,[5] in which the tropism/homing but not

* Address correspondence to dmhuang@nhri.org.tw; ycchenmd@ntu.edu.tw.

Received for review September 2, 2011 and accepted November 5, 2011.

Published online November 05, 2011
10.1021/nn2033902

the differentiation capacity is required for stem cells to efficiently deliver therapeutic genes, therefore suggesting an unexpected gain of therapeutic benefit of stem cells from the originally supposed deleterious impact of SPIO labeling.

In addition to the above observations, we have found an overexpression of epidermal growth factor (EGF) receptor (EGFR) in ferucarbotran-labeled hMSCs. Although EGF and the aberrant activation of EGFR, such as overexpression of EGFR in tumor cells including colon carcinoma, play key roles in cell proliferation, cell motility, cell adhesion, invasion, cell survival, and angiogenesis, which results in the development and progression of various tumors,[9] it has been demonstrated that EGFR-transfected bone marrow stroma cells exhibit enhanced migration toward gliomas,[10] suggesting a positive role of overexpressed EGFR in stem cells in tumor therapy.

In this study, we present a new strategy that leads the impact of SPIO nanoparticles on stem cell attributes to favor stem cell therapy. We tested our hypothesis that overexpression of EGFR induced by ferucarbotran labeling in hMSCs could block EGFR activation for tumor progression through the competitive binding of tumorous EGF, and therefore EGFR-overexpressed hMSCs themselves would serve as a therapeutic agent. We demonstrate that EGFR-overexpressed hMSCs not only exhibited induced tropism toward colon cancer cells but also diminished tumor cell proliferation and angiogenesis *in vitro* and *in vivo*, which results in effective cancer therapy.

RESULTS AND DISSCUSSION

Effect of Ferucarbotran-Labeled hMSCs on Tumor Growth *in Vivo*: Contribution of Ferucarbotran-Induced Overexpression of EGFR to Tumor Tropism of hMSCs. As mentioned above, a proof-of-concept tumor therapy study was derived from the observation of overexpression of EGFR in ferucarbotran-labeled hMSCs, as shown in Figure 1A. It has been shown that after internalization into cells, SPIO nanoparticles could be transferred to lysosomes, in which degradation of SPIO nanoparticles may occur and free iron (Fe) could be released into the cytoplasm.[2,4] We also showed that ferucarbotran labeling up-regulated the EGFR protein level but not the transcript and that DFO, an iron chelator, blocked ferucarbotran-evoked EGFR overexpression (Figure S1), suggesting that ferucarbotran could be internalized into cells via lysosomes and that lysosomal degradation of ferucarbotran is important in EGFR expression.

For this proof-of-concept tumor therapy study, we examined and compared the antitumor effects, as demonstrated by tumor size, of unlabeled and ferucarbotran-labeled hMSCs on sc colon cancer-bearing mice first. As previously reported, mesenchymal stem cells (MSCs) can exert an inhibitory effect on several tumors,[5,11−13] and we observed the intrinsic tumor-inhibition activity of the

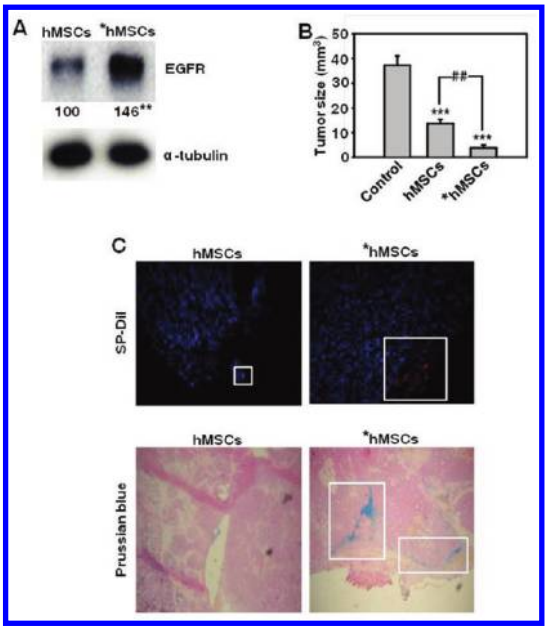

Figure 1. Evidence for ferucarbotran-labeled hMSCs' potent tumor tropism and superb antitumor activity. (A) Expression profiles of EGFR in unlabeled hMSCs (hMSCs) and ferucarbotran-labeled hMSCs (*hMSCs). α-Tubulin was the internal control. Results of Western blot shown are representative of four separate experiments. Densitometric analysis for the relative levels of the proteins of four separate experiments is indicated under each protein band ($p < 0.001$ as compared with hMSCs). (B) Tumor sizes of control mice, iv hMSCs-injected mice, and iv *hMSCs-injected mice ($n = 3-6$ per group) in a colon cancer model (***$p < 0.001$ as compared with control; $^{\#\#}p < 0.01$). (C) Immunohistological analyses of tumor tissues from iv hMSCs-injected mice and iv *hMSCs-injected mice. More *hMSCs migrated toward and accumulated around the tumor site than hMSCs, as demonstrated by SP-DiI staining (a small rectangle and a large rectangle in hMSCs group and *hMSCs group, respectively). Prussian blue staining shows the localization of *hMSCs (rectangles only in *hMSCs group). Section images were obtained with a 200× objective (Zeiss Axioskop 2).**

hMSCs (unlabeled hMSCs) in our study on colon tumor (HT-29) growth (Figure 1B). Interestingly, the antitumor activity was significantly elevated in ferucarbotran-labeled hMSCs-injected mice (Figure 1B). Because EGFR has been demonstrated to regulate migration in a variety of cells, we then examined whether the migration capacity was up-regulated accompanying EGFR overexpression and involved in the elevated antitumor activity of ferucarbotran-labeled hMSCs.

For histological examination, both unlabeled hMSCs and ferucarbotran-labeled hMSCs were labeled with fluorescent dye SP-DiI. Although the migration and localization of unlabeled hMSCs and ferucarbotran-labeled hMSCs around sc colon tumors could be hardly distinguished using a clinical 1.5-T MRI system *in vivo* (data not shown), the data from histological examinations, such as Prussian blue staining and fluorescence microscopic observation, demonstrated that ferucarbotran-labeled hMSCs exhibited enhanced tropism toward colon tumor than unlabeled hMSCs, suggesting a

contributive role of overexpressed EGFR in the induction of tumor tropism of ferucarbotran-labeled hMSCs (Figure 1C).

To confirm whether ferucarbotran-labeled hMSCs exhibited enhanced tumor tropism due to their overexpressed EGFR, an *in vitro* migration assay using a Transwell system was employed. Cells that had migrated from the top surface of the filters toward the lower surface of the filters were counted after staining with crystal violet. When serum-free medium was in the bottom chamber, neither unlabeled hMSCs nor ferucarbotran-labeled hMSCs in the top chamber could migrate downward (data not shown). As shown in Figure 2A, the migration capacity toward colon cancer cells in the bottom chamber significantly increased in ferucarbotran-labeled hMSCs compared with unlabeled hMSCs, suggesting a specific tropism of unlabeled hMSCs and ferucarbotran-labeled hMSCs, and a more potent tropism of ferucarbotran-labeled hMSCs than that of unlabeled hMSCs was observed. The treatment of EGFR inhibitor (AG) in the top chamber inhibited the migration of ferucarbotran-labeled hMSCs toward tumor cells in the bottom chamber (Figure 2B). Moreover, the attraction of recombinant human EGF (rhEGF) (in serum-free medium) in the bottom chamber for ferucarbotran-labeled hMSCs was inhibited by the treatment of EGF antibodies (Figure 2C). These results suggest that overexpressed EGFR in ferucarbotran-labeled hMSCs can be activated by tumor cell-secreted agonist(s), such as EGF, and are involved in the enhanced tumor tropism.

Effects of Ferucarbotran-Induced EGFR Overexpression of hMSCs on Tumor-Secreted EGF and Its Related Angiogenesis. On the basis of the above evidence we deduce that the elevated antitumor activity of ferucarbotran-labeled hMSCs on sc colon cancer, at least partly, resulted from stronger intrinsic antitumor activity of MSCs due to the overexpressed EGFR-enhanced tropism of more ferucarbotran-labeled hMSCs toward tumors. However, it could be logically hypothesized that there are other ways for ferucarbotran-labeled hMSCs with their overexpressed EGFR to accomplish superior antitumor activity because of the significant role of EGFR in a number of processes for tumor development and progression.[9] Once ferucarbotran-labeled hMSCs have approached tumor site(s), overexpressed EGFR of ferucarbotran-labeled hMSCs could further competitively bind to its cognate ligands, which were secreted by tumors, and thereby block the activation of EGFR signaling and consequent biological responses for tumor development and progression. Accordingly, two major responses, EGFR signaling-induced angiogenesis and stimulation of tumor growth, were investigated.

We focused tumor-secreted ligands on EGF and examined whether ferucarbotran-labeled hMSCs could capture tumor-secreted EGF to block EGFR signaling-induced angiogenesis. After HT-29 cells were grown in growth medium for 48 h, EGF was indeed secreted by HT-29 colon cancer cells into the culture supernatant (Figure 3A, control). After the incubation of the tumor cell culture supernatant with the same numbers of unlabeled hMSCs or ferucarbotran-labeled hMSCs, the amount of EGF in the supernatant was significantly decreased, especially in that of ferucarbotran-labeled hMSCs (Figure 3A). Moreover, pretreatment of ferucarbotran-labeled hMSCs with EGF peptides (EGF Pt) raised the amount of EGF to that treated with unlabeled hMSCs (Figure 3A). The data suggest ferucarbotran-labeled hMSCs with overexpressed EGFR could specifically capture tumor-secreted EGF more potently than unlabeled hMSCs.

To further examine the role of tumorous EGF in angiogenesis, an *in vivo* Matrigel plug assay was used. At day 7 of implantation of Matrigel plugs mixed with tumor cell culture supernatants (Figure 3B, control), the formation of hemorrhagic lesions in the isolated Matrigel pellets was evident by *ex vivo* observation (Figure 3B, control *vs* negative). The neovascularization process was significantly reduced in the Matrigel plugs mixed with unlabeled hMSCs-preincubated tumor cell culture supernatants (Figure 3B, hMSCs *vs* control) and more visibly blocked in the Matrigel plugs mixed with ferucarbotran-labeled hMSCs-preincubated tumor cell culture supernatants (Figure 3B, *hMSCs *vs* hMSCs). Quantification of vascularization by determination of hemoglobin content showed a greater inhibition of tumor cell culture supernatant-induced angiogenesis in ferucarbotran-labeled hMSCs-incubated Matrigel pellets than in that of incubation with unlabeled hMSCs (Figure 3C). The sections of Matrigels pellets were also stained with CD31 to determine the vascularization. Matrigel plugs mixed with unlabeled hMSCs- or ferucarbotran-labeled hMSCs-preincubated tumor cell culture supernatant showed a significantly lower angiogenesis than no treatment (control in Figure 3D and E). Microvessel density quantification as measured by fluorescence intensity of CD31 staining was significantly reduced in Matrigel pellets mixed with ferucarbotran-labeled hMSCs-preincubated tumor cell culture supernatant than in Matrigel pellets mixed with unlabeled hMSCs-preincubated tumor cell culture supernatant (Figure 3E). Histological observation (Figure 3D) and microvessel density quantification (Figure 3E) were consistent with hemoglobin content data. These results suggest that the secretion of EGF by tumor cells plays a role in angiogenesis and that the inhibitory effect of overexpressed EGFR on angiogenesis might be involved in superb antitumor activity of ferucarbotran-labeled hMSCs.

Effect of Ferucarbotran-Induced EGFR Overexpression of hMSCs on EGF-Stimulated Tumor Growth *in Vitro*. Since we have demonstrated that overexpressed EGFR of ferucarbotran-labeled hMSCs could capture and occupy tumor cell-secreted EGF and subsequently block tumor cell-induced angiogenesis,

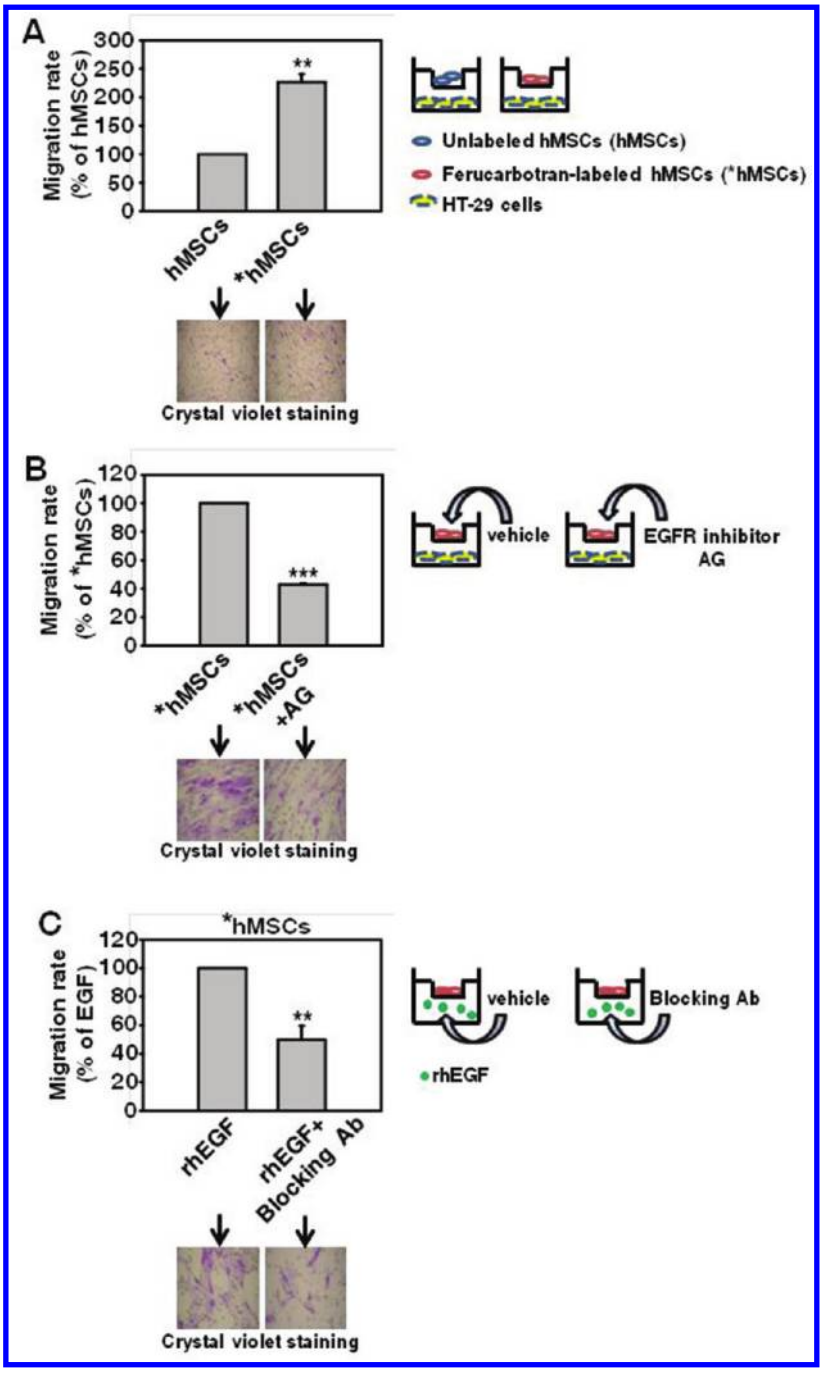

Figure 2. *In vitro* **migration capacities of unlabeled hMSCs (hMSCs) and ferucarbotran-labeled hMSCs (*hMSCs). (A) Migration activities of hMSCs and *hMSCs toward HT-29 cells. (B) Inhibitory effect of EGFR inhibitor AG on the migration of *hMSCs toward HT-29 cells. (C) Migratory effect of rhEGF and the effect of its blocking antibody on rhEGF-induced migration in *hMSCs. (B and C) Representative images of crystal violet staining are shown underneath the bars of each histogram. All data are expressed as mean ± standard error of three to four determinations (each in quadruplicate) (**$p < 0.01$; ***$p < 0.001$). The migration rate is expressed as the percentage variation of migrated cell number with respect to the corresponding control as 100%.**

we next examined whether the elimination of tumor cell-secreted EGF could prohibit its autocrine tumor cell growth.

To examine the growth effect of EGF on tumor cells, exogenous addition of rhEGF into fresh medium was first used. rhEGF at a high dose (50 ng/mL) showed a minor but significant growth promotion in tumor cells cultured with growth medium (Figure 4A). In contrast, rhEGF showed a marked and dose-dependent growth promotion in tumor cells cultured with serum-free medium (Figure 4B). When both growth medium and serum-free medium containing rhEGF were preincubated with the same numbers of unlabeled hMSCs or ferucarbotran-labeled hMSCs, no growth reduction was observed in tumor cells cultured with unlabeled hMSCs-treated or ferucarbotran-labeled hMSCs-treated growth medium (Figure 4C); however, the viability of

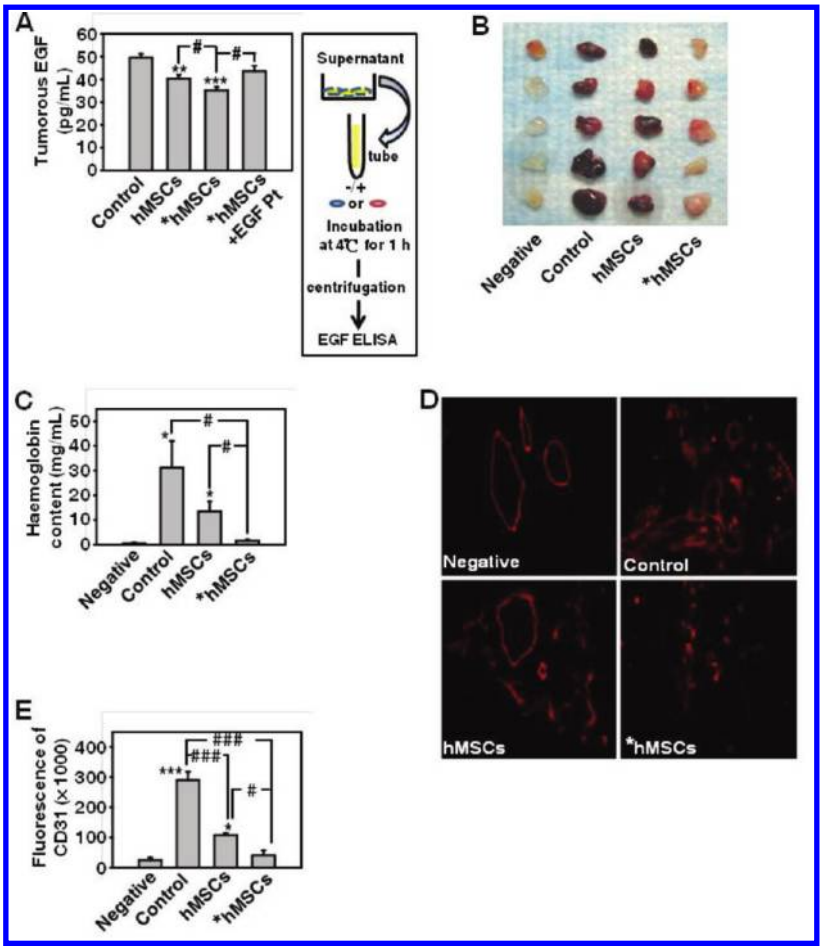

Figure 3. Effects of the captured binding of tumorous EGF by unlabeled hMSCs (hMSCs) and ferucarbotran-labeled hMSCs (*hMSCs) on *in vivo* angiogenesis. (A) Captured binding of tumorous EGF by hMSCs and *hMSCs. *hMSCs captured more EGF than hMSCs, and the treatment of EGF peptides (EGF Pt) prevented *hMSCs' captured binding of tumorous EGF ($p < 0.01$ and ***$p < 0.001$ as compared with respective control; $^{\#}p < 0.05$). (B) Matrigel plugs without (saline as negative) or with tumor cell supernatants were not pretreated (as control) or pretreated with hMSCs or *hMSCs and then implanted into mice (five for each group). After 7 days after the implantation of Matrigel plugs, formed Matrigel pellets were obtained from different mice and photographed. (C) Hemoglobin content of Matrigel pellets from part B (*$p < 0.05$ as compared with negative; $^{\#}p < 0.05$). (D) Immunofluorescent staining of Matrigel pellet sections with CD31 from part B. (E) Quantification of vasculature as an index of CD31 fluorescence intensity from part D. Areas of CD31 were measured in 8−10 images from each group (***$p < 0.001$ as compared with negative; $^{\#}p < 0.05$; $^{\#\#\#}p < 0.001$).**

tumor cells was significantly suppressed in both hMSCs-treated serum-free medium groups (Figure 4D). Moreover, the cell viability reduction was more significant in cells cultured with ferucarbotran-labeled hMSCs-treated serum-free medium than in that with unlabeled hMSCs-treated serum-free medium (Figure 4D). These results suggest that EGF plays an important role in autocrine tumor growth *in vivo* under specific conditions, such as starvation or the early stage of tumor development (carcinogenesis) and invasion (progression), needing a regional angiogenesis for a sufficient supply of energy resources for tumor cells.[14−16]

Next, to investigate whether tumorous EGF secreted in culture medium can indeed promote tumor cell growth, after HT-29 cells were cultured with serum-free medium for 4 h or with growth medium for 48 h to allow EGF secretion, both media were collected and incubated with unlabeled hMSCs or ferucarbotran-labeled hMSCs and then added to newly seeded HT-29 cells different from the cells used for secreting EGF. After incubation for 24 h for growth, the cell viabilities of HT-29 were determined. Interestingly, when cells were incubated in culture supernatant in growth media, the cell viability reduction was obviously observed in both unlabeled hMSCs-treated and ferucarbotran-labeled hMSCs-treated groups but still was more profoundly induced in the ferucarbotran-labeled hMSCs-treated group (Figure 4E). However, when cells were grown in culture supernatant in serum-free media, a minor but significant cell viability reduction was observed only in the ferucarbotran-labeled hMSCs-treated group (Figure 4F). We suggested that beside tumor-secreted EGF the presence of numerous tumorous factors (other growth factors, cellular metabolites, *etc.*) in the tumor cell culture supernatant medium affect the opposite action patterns of serum on cell viability in rhEGF-containing

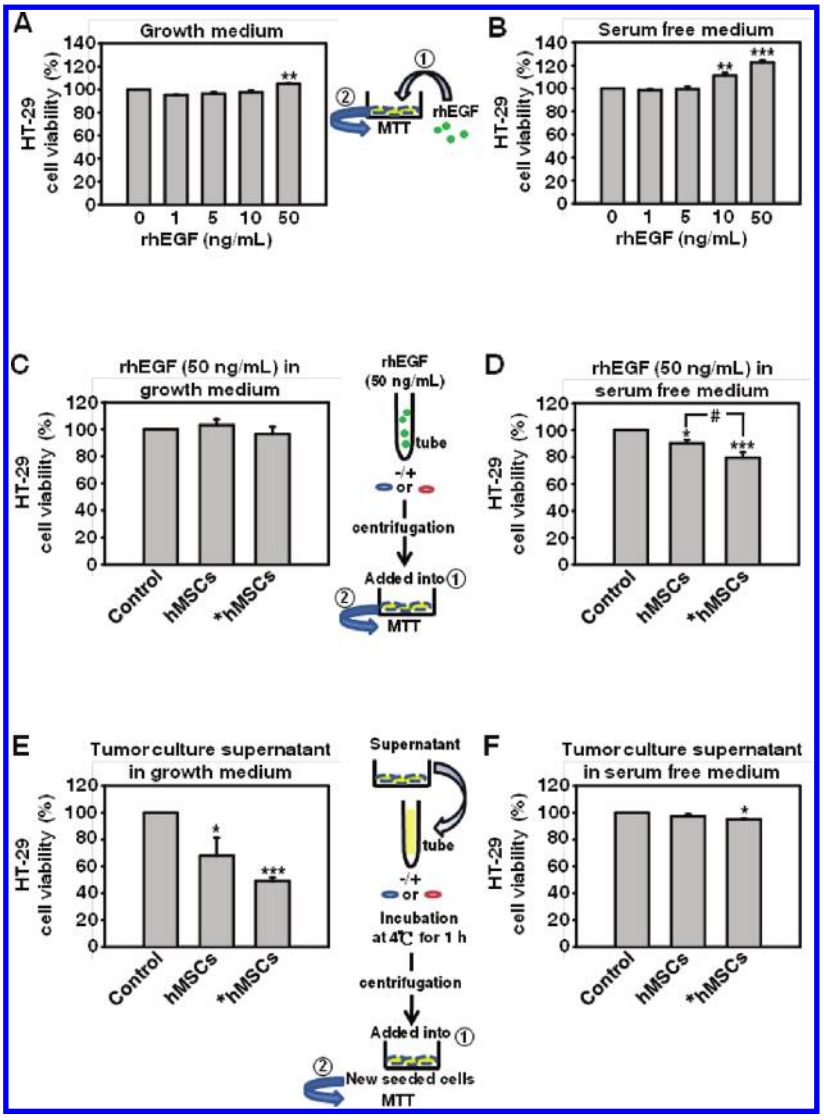

Figure 4. Effects of the captured binding of tumorous EGF by unlabeled hMSCs (hMSCs) and ferucarbotran-labeled hMSCs (*hMSCs) on *in vitro* cell growth. (A and B) Effects of rhEGF at various doses on HT-29 cell viability in growth medium (A) and serum-free medium (B). (C and D) Effects of captured binding of rhEGF by hMSCs and *hMSCs on HT-29 cell viability in growth medium (C) and serum-free medium (D). (E and F) Effects of captured binding of tumorous EGF by hMSCs and *hMSCs on HT-29 cell viability in growth medium (E) and serum-free medium (F). All data are expressed as mean ± standard error of three to seven determinations (each in quadruplicate) (*$p < 0.05$; **$p < 0.01$; ***$p < 0.001$ as compared with respective control; #$P < 0.05$). The data are expressed as the percentage variation of control cell viability as 100%.

medium (Figure 4C and D) and tumor cell culture supernatant medium (Figure 4E and F).

Taken together, the data suggest the possibility that ferucarbotran-labeled hMSCs with more EGFR expression than unlabeled hMSCs could more effectively inhibit tumor cell growth through occupying more autocrine-secreted EGF from tumor cells themselves, which also likely contributes to superb antitumor activity of ferucarbotran-labeled hMSCs on colorectal tumors in the study.

Effect of Ferucarbotran-Induced EGFR Overexpression of hMSCs on Tumorous Vascular Endothelia Growth Factor (VEGF). In addition to EGF, VEGF plays an important role in tumor angiogenesis, growth, and progression.[17] Moreover, the EGF/EGFR signaling pathway drives VEGF expression[18,19] and, conversely, EGFR inhibition can down-regulate VEGF expression in many tumor cell types and consequently tumor angiogenesis.[20,21] Therefore, we explored whether tumor-secreted VEGF would be diminished due to the captured elimination of tumorous EGF by ferucarbotran-induced EGFR overexpression of hMSCs.

To establish the positive role of EGF on driving VEGF expression in HT-29 cells, fresh media containing rhEGF were incubated without or with unlabeled hMSCs or ferucarbotran-labeled hMSCs and then used to treat cells to determine the effects of the captured elimination, if any, of rhEGF on tumorous VEGF expression. When growth medium and serum-free medium containing rhEGF were preincubated with the same numbers of unlabeled hMSCs or ferucarbotran-labeled hMSCs, tumorous

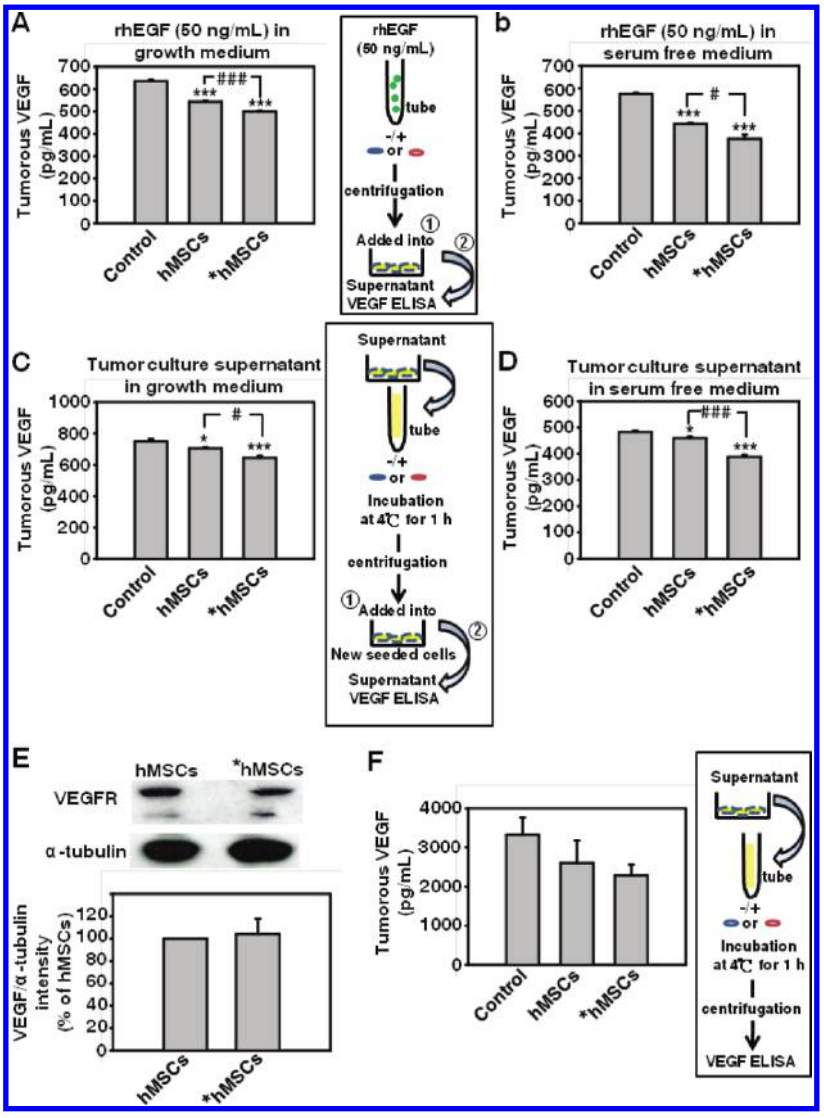

Figure 5. Effects of the captured binding of tumorous EGF by unlabeled hMSCs (hMSCs) and ferucarbotran-labeled hMSCs (*hMSCs) on tumorous VEGF expression. (A and B) Effects of captured binding of rhEGF by hMSCs and *hMSCs on tumorous VEGF expression in growth medium (A) and serum-free medium (B). (C and D) Effects of captured binding of tumorous EGF by hMSCs and *hMSCs on tumorous VEGF expression in growth medium (C) and serum-free medium (D). (A–D) All data are expressed as mean ± standard error of three to five determinations (each in quadruplicate) (*$p < 0.05$; ***$p < 0.001$ as compared with respective control; $^{\#}p < 0.05$; $^{\#\#, \#\#\#}p < 0.001$). (E) Expression profiles of VEGFR in hMSCs and *hMSCs. α-Tubulin was the internal control. Results of Western blot shown are representative of four separate experiments. Densitometric analysis for the relative level of VEGFR protein. Values represent mean ± standard error of four experiments. (F) Captured binding of tumorous VEGF by hMSCs and *hMSCs. No difference was observed between hMSCs-captured VEGF and *hMSCs-captured VEGF. Values represent mean ± standard error of three determinations (each in quadruplicate).

VEGF expression was obviously lower in both unlabeled hMSCs- and ferucarbotran-labeled hMSCs-treated groups; simultaneously, the expressions of tumorous VEGF were significantly weaker in HT-29 cells cultured with ferucarbotran-labeled hMSCs-treated media than in that with unlabeled hMSCs-treated media (Figure 5A and B), suggesting a driving role of EGF in VEGF expression in HT-29 cells in the study and an inhibitory effect of EGFR in hMSCs, especially overexpressed EGFR of ferucarbotran-labeled hMSCs, on EGF-induced VEGF expression.

Next, similar to the experimental conditions in Figure 4E and F, the media from 4 h serum-free culture or 48 h growth culture were incubated with unlabeled hMSCs or ferucarbotran-labeled hMSCs and then added to newly seeded HT-29 cells; however, VEGF secreted by HT-29 into 24 h culture supernatants was determined. As shown in Figure 5C and D, in both culture supernatants, the contents of tumorous VEGF were significantly lower in both unlabeled hMSCs-treated and ferucarbotran-labeled hMSCs-treated groups but were more markedly decreased in the ferucarbotran-labeled hMSCs-treated group.

To verify the contributive role of the captured elimination of tumorous EGF on VEGF expression in HT-29, we examined whether ferucarbotran-labeled hMSCs would overexpress VEGFR as well as whether

the decrease of VEGF in the culture supernatant resulted from the direct capture by overexpressed VEGFR of ferucarbotran-labeled hMSCs. Western blot showed no induced expression of VEGFR in ferucarbotran-labeled hMSCs (Figure 5E). These results have demonstrated that tumorous VEGF expression would be stimulated by rhEGF or tumorous EGF and then this expression could be inhibited by hMSCs' EGFR-captured elimination of EGF and that ferucarbotran-labeled hMSCs could more efficiently decrease tumorous VEGF expression than unlabeled hMSCs (Figure 5A–D). However, no difference in VEGFR expression (Figure 5E) suggested that the greater decrease of tumorous VEGF in the ferucarbotran-labeled hMSCs-treated groups (Figure 5C and D) was due to the direct capture of tumorous VEGF by hMSCs' VEGFR. Therefore, we examined the direct capture of tumorous VEGF by measuring the VEGF content in unlabeled hMSCs-treated or ferucarbotran-labeled hMSCs-treated cultured supernatant of tumor cells. Since the VEGF content in 4 h serum-free culture was minor, we determined the content of VEGF in 48 h growth medium. After the incubation of the tumor cell culture supernatant with the same numbers of unlabeled hMSCs or ferucarbotran-labeled hMSCs, VEGF contents were decreased in unlabeled hMSCs-treated and ferucarbotran-labeled hMSCs-treated supernatants; however, no significant decrease of VEGF between these two groups was observed (Figure 5F). These results demonstrate that ferucarbotran labeling can induce EGFR but not VEGFR expression in hMSCs and that both unlabeled hMSCs and ferucarbotran-labeled hMSCs can equally capture tumorous VEGF. Moreover, the data suggest that the more potent elimination of tumorous EGF by overexpressed EGFR of ferucarbotran-labeled hMSCs would result in EGF/EGFR signal blocking in tumor cells and consequent diminishing of VEGF expression.

CONCLUSIONS

The current study first verified that the labeling of ferucarbotran for cellular MRI can induce EFGR expression in hMSCs and furthermore demonstrated that the overexpressed EGFR contributed to the superb antitumor capacity of ferucarbotran-labeled hMSCs in a colon cancer model. After labeling with ferucarbotran, abundant expression of EGFR was induced on the hMSCs' surface, and EGFR was attracted by tumorous EGF to stimulate the tropism of ferucarbotran-labeled hMSCs toward colon cells. It is possible that due to their overexpressed EGFR, more ferucarbotran-labeled hMSCs can gather at the tumor site than unlabeled hMSCs to exert a more potent intrinsic antitumor activity. Moreover, when stem cells migrated to and around tumor cells, ferucarbotran-labeled hMSCs, with their overexpressed EGFR, can more effectively capture tumorous EGF than unlabeled hMSCs. Once much less EGF was available for tumor cells, EGF directly derived tumor cell growth and tumorous angiogenesis were immediately inhibited. The blockage of EGF-derived VEGF expression furthermore prohibited tumor progression and development. Taken together, the unexpected effect of ferucarbotran labeling on EGFR expression renders stem cells more favorable for the treatment of cancer. In summary, our work provides new thoughts on how the impacts of nanomaterials can be used for the application of nanotechnology to biomedicine.

MATERIALS AND METHODS

Materials. Mouse anti-EGFR antibody was from BD BioSciences. Rabbit anti-α-tubulin monoclonal antibody and VEGFR monoclonal antibody were from Cell Signaling Technologies and used at a dilution of 1:1000. Horseradish peroxidase (HRP)-conjugated secondary antibodies were obtained from Chemicon. Recombinant human EGF (rhEGF) and monoclonal antihuman EGF antibody were from R&D. EGFR peptide was from XXXXX (Santa Cruz, CA, USA). AG1478 as a tyrosine kinase inhibitor with a selectivity for the EGFR and potassium hexacyanoferrate(II) trihydrate iron were from Sigma. Superparamagnetic iron oxide nanoparticles, ferucarbotran (Resovist, Bayer Schering Pharma AG, Berlin, Germany), consist of SPIO nanoparticles coated with carboxydextran, which offers the complex a net negative charge and ensures stable dispersion of the nanoparticles within an aqueous environment.

Cell Culture. Human mesenchymal stem cells were isolated from bone marrow of normal donors as described previously,[22] with informed consent approved according to the procedures of the institutional review board. The hMSCs were cultured in regular growth medium consisting of low-glucose DMEM (GIBCO) supplemented with 10% fetal bovine serum (FBS) (HyClone), 100 U/mL penicillin, and 100 μg/mL streptomycin. All cultures were kept in an atmosphere of 5% CO_2 and 95% air at 37 °C. All experiments were carried out with hMSCs of the fifth to seventh passage. HT-29 (colon adenosarcoma) cells were cultured in low-glucose DMEM supplemented with 10% fetal bovine serum (GIBCO) and were maintained in a 5% CO_2 atmosphere at 37 °C.

hMSCs Labeling with SP-DiI and Ferucarbotran. The fluorescent dye SP-DiI (dilution, 1:1000, Molecular Probes) was used to label the hMSCs at 37 °C for 48 h in growth medium. After fluorescent labeling, cells were rinsed with 1 × PBS and then incubated or not with ferucarbotran (300 μg/mL) in serum-free medium for 60 min at 37 °C. Ferucarbotran-labeled hMSCs were denoted as *hMSCs.

Western Blot Analysis. hMSCs (0.6×10^6 cells) were incubated with regular cultured medium in 100 mm dishes. The hMSCs were treated with ferucarbotran (300 μg/mL) in serum-free medium at 37 °C for 60 min. After treatment cells were rinsed with ice-cold 1× PBS and were lysed by the addition of lysis buffer (25 mM HEPES, pH 7.5, 150 mM NaCl, 1% Igepal CA-630, 10 mM $MgCl_2$, 1 mM EDTA, 2% glycerol, 1 μM phenylmethylsulfonyl fluoride, 1 μg/mL leupeptin, and 10 μg/mL aprotinin) for 60 min at 4 °C. The suspensions were centrifuged at 15700*g* for 20 min at 4 °C. The protein concentration of the supernatant was assessed by the Bio-Rad protein assay kit.

Proteins were separated by electrophoresis in a 10% polyacrylamide gel and transferred to a polyvinylidene difluoride membrane. Then they were incubated at room temperature in 0.1% Tween 20 with TBS plus 5% bovine serum albumin (BSA) for 60 min. Antibodies were added to TBST containing 1% BSA and incubated with the membranes at 4 °C. Membranes were then washed three times in TBST, for 10 min each time. After

washing, HRP-conjugated anti-rabbit (AP132; dilution 1:5000, Chemicon) or anti-mouse (AP124P; dilution, 1:5000, Chemicon) antibodies were incubated with membranes for 60 min at room temperature. After washing, the membranes were developed using the Immobilon Western chemiluminescent HRP substrate kit (Millipore).

Tropism and Antitumor Activity of hMSCs *in Vivo*. Pathogen-free, female Balb-c nude mice (7 weeks old) were obtained from National Laboratory Animal Center of Taiwan. Mice were housed with a 12 h light/12 h dark cycle. Mice weighing 18−20 g were used for the experiments described below. To evaluate the migration of hMSCs toward tumor, HT-29 cells were administered as a suspension at 1.0×10^6 cells in 100 μL of PBS sc into the flank of mice. After 10 days, the suspension of 1.0×10^6 hMSCs with the indicated treatments in 200 μL of PBS/each animal was injected iv into the lateral tail vein for the systemic administration. Mice were euthanized and sacrificed on day 17 after tumor cell implantation. Tumor volume was measured by caliper and calculated according to the formuls volume = length $\times$ width^2/2. Then tumors were harvested and their iron contents and the localization of hMSCs were immunohistochemically examined.

Immunohistochemistry (IHC), Prussian Blue Staining, and Fluorescent Microscopy Analysis of hMSC Tropism toward Tumor. To detect hMSCs by fluorescence, hMSCs were labeled with SP-DiI. Tumors were frozen, and SP-DiI-labeled hMSCs were detected on fresh sections (8 μm) of tumor samples under a fluorescent microscope.

Alternatively, tumor sections (8 μm) were air-dried for 10 min at room temperature. Samples were incubated in a solution containing 10% potassium hexacyanoferrate(II) trihydrate iron and 20% hydrochloric acid for 20 min at room temperature. After 20 min incubation, samples were washed twice with 1$\times$ PBS, counterstained with eosin Y solution (Sigma) for 2 min, and observed under the microscope.

***In Vitro* Migration of hMSCs.** Studies on chemotactic migration of hMSCs were performed using the Costar Transwell chamber system (24-well; Costar, Pleasanta, CA, USA) with membrane filters with a pore size of 8 μm. Samples, each containing 4.0×10^4 cells in 200 μL of growth medium, were added to the upper compartments (top chambers or inserts) and incubated overnight for seeding. On the other hand, the lower compartments (bottom chambers) were added with HT-29 cells at 2.0×10^5 cells/600 μL of 10% FBS-containing DMEM per chamber and incubated overnight (Figure 2A and B) or filled with 600 μL of rhEGF-containing medium per chamber (Figure 2C). The cells in the upper compartments were then labeled with Resovist (300 μg/mL) in serum-free medium at 37 °C for 60 min. After labeling, the upper compartments were transferred to the bottom chambers. After the indicated treatments as shown in schemes appendixed with respective figures, the migration chambers were incubated for 24 h at 37 °C in a humidified air atmosphere with 5% CO_2. After incubation, cells on the top surface of the filters of the upper compartments were wiped off with cotton swabs. Cells that had migrated toward the lower surface of the filters were counted after staining with 0.5% crystal violet (Sigma). Four replicates of each sample were counted. Each migration experiment was performed in triplicate. The migration rate was expressed as the percentage variation of migrated cell number with respect to the corresponding control as 100%.

***In Vivo* Angiogenesis Assay.** HT-29 cells were seeded as 1.0×10^6 cells per dish in 100 mm dishes with 6 mL of growth media overnight and allowed to grow for 48 h. The HT-29 supernatants (1 mL each sample) were incubated with unlabeled hMSCs or ferucarbotran-labeled hMSCs (1.0×10^5 cells per condition) for 60 min at 4 °C. After incubation, cells were spun-down at 4 °C. The supernatants (133 μL each reaction) were mixed with heparin (7 μL, final concentration of 50 U) and Matrigel (560 μL, Becton Dickinson, USA) to a final volume of 700 μL. Mice were randomized into four groups (five mice per group) and sc injected with 500 μL of the Matrigel mixture plug near the abdominal midline for each mouse as follows: Matrigel plug mixed with heparin as a negative control (negative), Matrigel plug mixed with HT-29 supernatant and heparin (control), Matrigel plug mixed with hMSCs-pretreated HT-29 supernatant and heparin (hMSCs), Matrigel plug mixed with ferucarbotran-labeled hMSCs-pretreated HT-29 supernatant and heparin (*hMSCs). Mice were euthanized on day 7 after Matrigel implantation to harvest Matrigel pellets for determining the hemoglobin content using a Drabkin reagent kit (Sigma) and for examining neovascularization immunohistochemically.

Hemoglobin Assay and Immunohistochemistry for Neovascularization. The Matrigel pellets were collected in a 1.5 mL Eppendorf containing 1 mL of 1$\times$ PBS, vortex-mixed to elute the hemoglobin, and then centrifuged at 9300*g* for 10 min at 4 °C. By pipet 100 μL of supernatant was mixed with 500 μL of Drabkin's reagent at room temperature for 30 min, and the absorbance at 540 nm was measured using a microplate reader.

To examine the neovascularization in the xenografts, sections of Matrigel (8 μm) were obtained from OCT (Sakura Tissue-Tek)-embedded frozen tissues using 2-methylbutane (Sigma), then were kept at −80 °C. Sections were fixed in cold acetone for 5 min at −20 °C and washed with 1$\times$ PBS one time for 3 min. Sections were then stained with rat anti-mouse CD31-PE (#553373) and rat IgG2a isotype control (#553930) (dilution, 1:50 in PBS, BD BioSciences) for 2 h at 37 °C (80 μL per slice). After the samples were rinsed three times with 1$\times$ PBS for 5 min, immunofluorescent images were obtained with a 200$\times$ objective (Zeiss Axioskop 2). Microvessel density quantification was measured by calculating the pixels corresponding to the fluorescence intensity of CD31 staining (MetaXpress, Molecular Devices, USA), on adjusting the threshold and excluding nonvessel stray pixels.

EGF and VEGF ELISA. To examine whether unlabeled hMSCs and ferucarbotran-labeled hMSCs can capture tumorous EGF and VEGF (Figures 3A and 5F), HT-29 cells were seeded at 1.0×10^6 cells per dish in 100 mm dishes with 6 mL of growth medium overnight and allowed to grow for 48 h; then the HT-29 supernatants (1 mL each sample) were incubated with unlabeled hMSCs or ferucarbotran-labeled hMSCs (1.0×10^5 cells per condition) for 60 min at 4 °C. Then the cell supernatants were spun-down for a commercially available enzyme-linked immunosorbent assay kit (ELISA; R&D Systems) for human recombinant EGF or VEGF.

To examine the effect of rhEGF (Figure 5A and B) on tumorous VEGF expression, 1 mL of fresh medium containing rhEGF (50 ng/mL) was incubated with unlabeled hMSCs or ferucarbotran-labeled hMSCs (1.0×10^5 cells per condition) for 60 min at 4 °C. After incubation, cells were spun-down, and supernatants were added into newly seeded tumor cells for 24 h. To examine the effect of tumorous EGF (Figure 5C and D) on tumorous VEGF expression, HT-29 cells were seeded at 1.0×10^6 cells per dish in 100 mm dishes with 6 mL of growth medium overnight and allowed to grow for 48 h or incubated with serum-free medium for 4 h. The HT-29 supernatants in serum-free or growth media (1 mL each sample) were incubated with unlabeled hMSCs or ferucarbotran-labeled hMSCs (1.0×10^5 cells per condition) for 60 min at 4 °C. Then the cells were spun-down and the supernatants were collected and added into newly seeded tumor cells for 24 h. Then all cell supernatants in both conditions were spun-down for a commercially available enzyme-linked immunosorbent assay kit (ELISA; R&D Systems) for human recombinant VEGF.

MTT Assay. To examine the effect of rhEGF on cell growth, HT-29 cells were seeded in 24-well plates at 1.0×10^5 cells per well overnight and then incubated with rhEGF at various concentrations in serum-free or growth media for 24 h (as shown in schemes appendixed with Figure 4A and B). To examine whether unlabeled hMSCs and ferucarbotran-labeled hMSCs can capture rhEGF and then block EGF-dependent cell growth, fresh serum-free and growth media containing rhEGF (50 ng/mL) were incubated with unlabeled hMSCs and ferucarbotran-labeled hMSCs for 60 min at 4 °C. Then the cells were spin-down, and the supernatants were collected and added into newly seeded tumor cells in 24-well plates at 1.0×10^5 cells per well for 24 h (as shown in schemes appendixed with Figure 4C and D). To examine the role of tumorous EGF on autocrine cell growth, HT-29 cells were seeded at 1.0×10^6 cells per dish in 100 mm dishes with 6 mL of growth medium overnight and allowed to grow in growth medium for 48 h or incubated with serum-free

medium for 4 h. Then the cell supernatants were collected and incubated with hMSCs or ferucarbotran-labeled hMSCs (1.0×10^5 cells in 1 mL of supernatant per condition) for 60 min at 4 °C. After incubation, cells were spun-down, and the supernatants were collected and added into newly seeded tumor cells in 24-well plates at 1.0×10^5 cells per well for 24 h (as shown in schemes appendixed with Figure 4E and F). After the indicated treatments as shown in schemes appendixed with respective figures, cells were incubated with fresh serum-free medium containing MTT (0.5 mg/mL) for 60 min at 37 °C. The dark blue formazan dye generated by the live cells was proportional to the number of live cells, and the absorbance at 570 nm was measured using a microplate reader.

Statistical Analysis. Data are presented as the mean ± standard error of the mean for the indicated numbers of separate experiments. The results were compared using Student's *t* test in the case of two groups for comparison. For more than two groups, ANOVA was used for experiment significance, and we used Tukey's Honestly Significant difference test for *post hoc* analysis. We used freeware for these computations (R version 2.11.1). Statistical significance was assigned if the probability value (*p*) was less than 0.05.

Acknowledgment. This study was supported by grants from the National Health Research Institutes (NHRI) (NM-099-PP-02, NM-99-PP-09, NM-100-PP02, and NM-100-PP-09) and the National Science Council (99-2320-B-400-002-MY3 and 99-2314-B-303-012-MY3), both of Taiwan.

Supporting Information Available: Possible mechanism study of ferucarbotran-induced overexpression of EGFR is available. This material is available free of charge *via* the Internet at http://pubs.acs.org.

REFERENCES AND NOTES

1. Kostura, H.; Kraitchman, D. L.; Mackay, A. M.; Pittenger, M. F.; Bulte, J. W. Feridex Labeling of Mesenchymal Stem Cells Inhibits Chondrogenesis but Not Adipogenesis or Osteogenesis. *NMR Biomed.* **2004**, *17*, 513–517.
2. Arbab, A. S.; Yocum, G. T.; Rad, A. M.; Khakoo, A. Y.; Fellowes, V.; Read, E. J.; Frank, J. A. Labeling of Cells with Ferumoxides-Protamine Sulfate Complexes Does Not Inhibit Function or Differentiation Capacity of Hematopoietic or Mesenchymal Stem Cells. *NMR Biomed.* **2005**, *18*, 553–559.
3. Huang, D. M.; Hsiao, J. K.; Chen, Y. C.; Chien, L. Y.; Yao, M.; Chen, Y. K.; Ko, B. S.; Hsu, S. C.; Tai, L. A.; Cheng, H. Y.; *et al*. The Promotion of Human Mesenchymal Stem Cell Proliferation by Superparamagnetic Iron Oxide Nanoparticles. *Biomaterials* **2009**, *30*, 3645–3651.
4. Chen, Y. C.; Hsiao, J. K.; Liu, H. M.; Lai, I. Y.; Yao, M.; Hsu, S. C.; Ko, B. S.; Chen, Y. C.; Yang, C. S.; Huang, D. M. The Inhibitory Effect of Superparamagnetic Iron Oxide Nanoparticle (Ferucarbotran) on Osteogenic Differentiation and Its Signaling Mechanism in Human Mesenchymal Stem Cells. *Toxicol. Appl. Pharmacol.* **2010**, *245*, 272–279.
5. Chien, L. Y.; Hsiao, J. K.; Hsu, S. C.; Yao, M.; Lu, C. W.; Liu, H. M.; Chen, Y. C.; Yang, C. S.; Huang, D. M. *In Vivo* Magnetic Resonance Imaging of Cell Tropsim, Trafficking Mechanism, and Therapeutic Impact of Human Mesenchymal Stem Cells in a Murine Glioma Model. *Biomaterials* **2011**, *32*, 3275–3284.
6. Yang, C. Y.; Hsiao, J. K.; Tai, M. F.; Chen, S. T.; Cheng, H. Y.; Wang, J. L.; Liu, H. M. Direct Labelling of hMSC with SPIO: The Long-Term Influence on Toxicity, Chondrogenic Differentiation Capacity, and Intracellular Distribution. *Mol. Imaging Biol.* **2011**, *13*, 443–451.
7. Kim, H. S.; Oh, S. Y.; Joo, H. J.; Son, K. R.; Song, I. C.; Moon, W. K. The Effects of Clinically Used MRI Contrast Agents on the Biological Properties of Human Mesenchymal Stem Cells. *NMR Biomed.* **2010**, *23*, 514–522.
8. Balakumaran, A.; Pawelczyk, E.; Ren, J.; Sworder, B.; Chaudhry, A.; Sabatino, M.; Stroncek, D.; Frank, J. A.; Robey, P. G. Superparamagnetic Iron Oxide Nanoparticles Labelling of Bone Marrow Stromal (Mesenchymal) Cells Does Not Affect Their "Stemness". *PLoS ONE* **2010**, *5*, e11462.
9. Woodburn, J. R. The Epidermal Growth Factor Receptor and Its Inhibition in Cancer Therapy. *Pharmacol. Ther.* **1999**, *82*, 241–250.
10. Sato, H.; Kuwashima, N.; Sakaida, T.; Hatano, M.; Dusak, J. E.; Fellows-Mayle, W. K.; Papworth, G. D.; Watkins, S. C.; Gambotto, A.; Pollack, I. F.; *et al*. Epidermal Growth Factor Receptor-Transfected Bone Marrow Stromal Cells Exhibit Enhanced Migratory Response and Therapeutic Potential Against Murine Tumors. *Cancer Gene Ther.* **2005**, *12*, 757–768.
11. Nakamura, K.; Ito, Y.; Kawano, Y.; Kurozumi, K.; Kobune, M.; Tsuda, H.; Bizen, A.; Honmou, O.; Niitsu, Y.; Hamada, H. Antitumor Effect of Genetically Engineered Mesenchymal Stem Cells in a Rat Glioma Model. *Gene Ther.* **2004**, *11*, 1155–1164.
12. Khakoo, A. Y.; Pati, S.; Anderson, S. A.; Reid, W.; Elshal, M. F.; Rovira, I. I.; Nguyen, A. T.; Malide, D.; Combs, C. A.; Hall, G.; *et al*. Human Mesenchymal Stem Cells Exert Potent Antitumorigenic Effects in A Model of Kaposi's Sarcoma. *J. Exp. Med.* **2006**, *230*, 1235–1247.
13. Qiao, L.; Xu, Z.; Zhao, T.; Zhao, Z.; Shi, M.; Zhao, R. C.; Ye, L.; Zhang, X. Suppression of Tumorigenesis by Human Mesenchymal Stem Cells in a Hepatoma Model. *Cell Res.* **2008**, *18*, 500–507.
14. Ruck, A.; Paulie, S. The Epidermal Growth Factor Receptor Is Involved in Autocrine Growth of Human Bladder Carcinoma Cell Lines. *Anticancer Res.* **1997**, *17*, 1925–1931.
15. Yamamoto, N.; Mammadova, G.; Song, R. X.; Fukami, Y.; Sato, K. Tyrosine Phosphorylation of p145met Mediated by EGFR and Src Is Required for Serum-Independent Survival of Human Bladder Carcinoma Cells. *J. Cell Sci.* **2006**, *119*, 4623–4633.
16. Ruan, W. J.; Lai, M. D. Autocrine Stimulation in Colorectal Carcinoma (CRC): Positive Autocrine Loops in Human Colorectal Carcinoma and Applicable Significance of Blocking the Loops. *Med. Oncol.* **2004**, *21*, 1–8.
17. Herbst, R. S.; Johnson, D. H.; Mininberg, E.; Carbone, D. P.; Henderson, T.; Kim, E. S.; Blumenschein, G., Jr.; Lee, J. J.; liu, D. D.; Truong, M. T.; *et al*. Phase I/II Trial Evaluating the Anti-Vascular Endothelial Growth Factor Monoclonal Antibody Bevacizumab in Combination with the HER-1/Epidermal Growth Factor Receptor Tyrosine Kinase Inhibitor Erlotinib for Patients with Recurrent Non-Small-Cell Lung Cancer. *J. Clin. Oncol.* **2005**, *23*, 2544–2555.
18. Niu, G.; Wright, K. L.; Huang, M.; Song, L.; Haura, E.; Turkson, J.; Zhang, S.; Wang, T.; Sinibaldi, D.; Coppola, D.; *et al*. Constitutive Stat3 Activity Up-Regulates VEGF Expression and Tumor Angiogenesis. *Oncogene* **2002**, *21*, 2000–2008.
19. Zhong, H.; Chiles, K.; Feldser, D.; Laughner, E.; Hanrahan, C.; Georgescu, M. M.; Simons, J. W.; Semenza, G. L. Modulation of Hypoxia-Inducible Factor 1Alpha Expression by the Epidermal Growth Factor/Phosphatidylinositol 3-Kinase/PTEN/AKT/FRAP Pathway in Human Prostate Cancer Cells: Implications for Tumor Angiogenesis and Therapeutics. *Cancer Res.* **2000**, *60*, 1541–1545.
20. Ciardiello, F.; Tortora, G. A Novel Approach in The Treatment of Cancer: Targeting The Epidermal Growth Factor Receptor. *Clin. Cancer Res.* **2001**, *7*, 2958–2970.
21. Pore, N.; Jiang, Z.; Gupta, A.; Cerniglia, G.; Kao, G. D.; Maity, A. EGFR Tyrosine Kinase Inhibitors Decrease VEGF Expression by Hypoxia-Inducible Factor (HIF)-1-Independent and HIF-1-Dependent Mechanisms. *Cancer Res.* **2006**, *66*, 3197–3204.
22. Huang, D. M.; Hung, Y.; Ko, B. S.; Hsu, S. C.; Chen, W. H.; Chien, C. L.; Tsai, C. P.; Kuo, C. T.; Kang, J. C.; Yang, C. S.; *et al*. Highly Efficient Cellular Labeling of Mesoporous Nanoparticles in Human Mesenchymal Stem Cells: Implication for Stem Cell Tracking. *FASEB J.* **2005**, *19*, 2014–2016.